

This article was downloaded by:

On: 23 January 2011

Access details: *Access Details: Free Access*

Publisher *Taylor & Francis*

Informa Ltd Registered in England and Wales Registered Number: 1072954 Registered office: Mortimer House, 37-41 Mortimer Street, London W1T 3JH, UK



## Journal of Coordination Chemistry

Publication details, including instructions for authors and subscription information:

<http://www.informaworld.com/smpp/title~content=t713455674>

### Synthesis, crystal structure, electrochemical and magnetic properties of dinuclear complexes with strong electron-drawing groups in the diphenoxo-tetraaza macrocyclic ligand

Lei Chen<sup>a</sup>; Jun-Lin Bai<sup>a</sup>; Hong Zhou<sup>a</sup>; Zhi-Quan Pan<sup>a</sup>; Qi-Mao Huang<sup>a</sup>; You Song<sup>b</sup>

<sup>a</sup> Hubei Key Laboratory of Chemical Reactor and Green Chemical Technology, Wuhan Institute of Chemical Technology, Wuhan 430073, P. R. China <sup>b</sup> Department of Chemistry, Hebei North University, Zhangjiakou, 075131, P. R. China

**To cite this Article** Chen, Lei , Bai, Jun-Lin , Zhou, Hong , Pan, Zhi-Quan , Huang, Qi-Mao and Song, You(2008)

'Synthesis, crystal structure, electrochemical and magnetic properties of dinuclear complexes with strong electron-drawing groups in the diphenoxo-tetraaza macrocyclic ligand', *Journal of Coordination Chemistry*, 61: 9, 1412 – 1422

**To link to this Article:** DOI: 10.1080/00958970701579274

**URL:** <http://dx.doi.org/10.1080/00958970701579274>

PLEASE SCROLL DOWN FOR ARTICLE

Full terms and conditions of use: <http://www.informaworld.com/terms-and-conditions-of-access.pdf>

This article may be used for research, teaching and private study purposes. Any substantial or systematic reproduction, re-distribution, re-selling, loan or sub-licensing, systematic supply or distribution in any form to anyone is expressly forbidden.

The publisher does not give any warranty express or implied or make any representation that the contents will be complete or accurate or up to date. The accuracy of any instructions, formulae and drug doses should be independently verified with primary sources. The publisher shall not be liable for any loss, actions, claims, proceedings, demand or costs or damages whatsoever or howsoever caused arising directly or indirectly in connection with or arising out of the use of this material.

## Synthesis, crystal structure, electrochemical and magnetic properties of dinuclear complexes with strong electron-drawing groups in the diphenoxo-tetraaza macrocyclic ligand

LEI CHEN<sup>†</sup>, JUN-LIN BAI<sup>†</sup>, HONG ZHOU<sup>†</sup>, ZHI-QUAN PAN<sup>\*†</sup>,  
QI-MAO HUANG<sup>†</sup> and YOU SONG<sup>‡</sup>

<sup>†</sup>Hubei Key Laboratory of Chemical Reactor and Green Chemical Technology, Wuhan Institute of Chemical Technology, Wuhan 430073, P. R. China

<sup>‡</sup>Department of Chemistry, Hebei North University, Zhangjiakou, 075131, P. R. China

(Received 29 November 2006; in final form 24 May 2007)

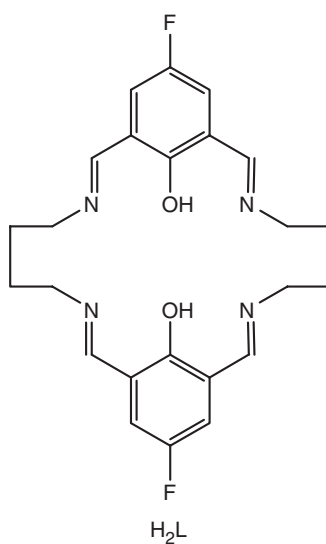
Three symmetrical macrocyclic dinuclear complexes  $[M_2L(H_2O)_n](ClO_4)_2$  ( $M^{2+} = Cu^{2+}, Ni^{2+}, Mn^{2+}$  and  $n = 0, 2$ ) have been synthesized by cyclocondensation between 2,6-diformyl-4-fluorophenol and 1,4-diaminobutane in the presence of  $M^{2+}$  cations. The crystal structure of  $[Cu_2L](ClO_4)_2$  was determined by X-ray diffraction techniques. The electronic and magnetic properties of the complexes were studied by cyclic voltammetry and magnetic susceptibility. The results confirm that the complexes obtain electrons easily and there are very strong antiferromagnetic couplings between two copper(II) ions in  $[Cu_2L](ClO_4)_2$ . The strong electron-drawing groups of fluorine attached to the phenyl ring of a macrocyclic complex enhances the antiferromagnetic exchange of the complex and makes it more easily reduced than its analogs.

**Keywords:** Crystal structure; Electrochemistry; Dinuclear macrocyclic complexes; Magnetism

### 1. Introduction

Coordination chemistry of macrocyclic ligands has attracted attention in [1–4] with design and synthesis of macrocyclic ligands important with diphenoxo-bridged ligands having powerful coordinating interaction with transition metal ions [5–8]. A number of diphenoxo-bridged macrocyclic complexes have been studied for the relationship between structure and properties such as magnetism and electrochemistry [9–12]. The cavity sizes of the coordinated metal ions in the complexes affect the electronic and magnetic properties of the complexes [13]. In our previous study [14], we found that alteration of the groups in the phenyl ring change the electron density in the C=N bond, changing the susceptibility of the macrocyclic complexes to attack by protons in solution and also affecting the ability of the metal ions to accept electrons [15]. Complexes with an F atom as substituted group on the phenyl in the diphenoxo-bridged macrocyclic complexes is less reported, and a new macrocyclic ligand ( $H_2L$ , scheme 1) derived from the 2+2 cyclocondensation

\*Corresponding author. Fax: +86-27-8719-4465. Email: zhiqpan@163.com

Scheme 1. The structure of H<sub>2</sub>L.

between 2,6-diformyl-4-fluorophenol and 1,4-diaminobutane and its complexes,  $[M_2L(H_2O)_n](ClO_4)_2$ , ( $M = Cu, Ni, Mn; n = 0, 2$ ) were synthesized, and the structures, electronic, magnetic properties, as well as stability of the complexes were studied to further understand the effect of the substituted groups on the structure of macrocyclic complexes.

## 2. Experimental

### 2.1. Materials

All solvents and chemicals were of analytical grade and used as received, except methanol, which was dried by general method. 2,6-Diformyl-4-fluorophenol was prepared according to the literature method [16].

### 2.2. Physical measurements

IR spectra were measured using KBr disc on a Vector 22 FT-IR spectrophotometer. Far-infrared spectra were recorded on a Nexus FT-IR spectrophotometer; frequencies were calibrated with polystyrene film. Nujol mulls were used for solid-state spectra. The contents of metals in complexes were determined by conductometric titration. The fluorine contents in the complexes were determined by oxygen flask combustion method. The samples were decomposed in oxygen flasks at 700°C and HF was absorbed in a solution of sodium hydroxide. Cerium nitrate was added to the solution, followed by ethanol. Excessive cerium ion was titrated with EDTA using mixed indicator of xylenol-orange tetrasodium and methylene blue. Thermoanalyses of the complexes were performed on a SDT 2960 TA thermoanalyzer under an argon atmosphere at

a rate of  $10^{\circ}\text{C min}^{-1}$ . Electrospray mass spectra (ES-MS) were determined on a Finnigan LCQ ES-MS mass spectrograph using methanol as the mobile phase with a sample concentration of about  $1.0\text{ mmol dm}^{-3}$ . The diluted solution was electrosprayed at a flow rate of  $5 \times 10^{-6}\text{ dm}^3\text{ min}^{-1}$  with a needle voltage of  $+4.5\text{ kV}$ . The temperature of the heated capillary in the interface was  $200^{\circ}\text{C}$  and a fuse silica sprayer was used.

The magnetic susceptibility of a crystalline-powdered sample was measured on a SQUID-based magnetometer in the temperature range  $1.78 \sim 300\text{ K}$ , and diamagnetic corrections were made using Pascal's constants. Cyclic voltammogram measurements were run on a CHI Model 750B electrochemical analyzer in DMF solution containing tetra(*n*-butyl)ammonium perchlorate (TBAP) as the supporting electrolyte. A three-electrode cell equipped with a glassy carbon-working electrode, a platinum wire as the counter electrode, and an Ag/AgCl electrode as the reference electrode was used. Scanning rates were in the range  $20 \sim 200\text{ mV s}^{-1}$ . The solution was deaerated for 15 min before measuring. Half-wave potentials were calculated approximately from  $(E_{\text{pa}} + E_{\text{pc}})/2$ , and the measured error was  $\pm 2\text{ mV}$ .

### 2.3. Crystal structure determination

Diffraction intensity data were collected on a SMART-CCD area-detector diffractometer at  $293\text{ K}$  using graphite monochromatic Mo- $K\alpha$  radiation ( $\lambda = 0.71073\text{ \AA}$ ). Data reduction and cell refinement were performed by SMART and SAINT Programs [17]. The structure was solved by direct methods (Bruker SHELXTL) and refined on  $F^2$  by full-matrix least squares (Bruker SHELXTL) using all unique data [18]. The non-H atoms in the structure were treated as anisotropic. Hydrogen atoms were located geometrically and refined in riding mode.

### 2.4. Preparation of the complexes

**[Cu<sub>2</sub>L](ClO<sub>4</sub>)<sub>2</sub> (1).** To a refluxing solution of 2,6-diformyl-4-fluorophenol (0.5 mmol, 0.084 g) in absolute methanol (15 mL) was added a solution of hydrated copper acetate (0.25 mmol, 0.05 g). The solution was stirred vigorously while a methanolic solution (15 mL) of 1,4-diaminobutane (0.5 mmol, 0.044 g) was slowly added. After addition, the resulting solution turned bright green, and triethylamine (*ca.* 1 mL) was added following reflux for 6 h. Hydrated copper perchlorate (0.25 mmol, 0.093 g) was added to the above solution, and the solution stirred for 4 h, and then ether (50 mL) was added to precipitate the product. The precipitate was filtered off, washed with ether, and dried in air (yield 0.075 g, 55%). Anal.: found: Cu, 16.58; F, 5.01; Calcd for C<sub>24</sub>H<sub>24</sub>N<sub>4</sub>F<sub>2</sub>Cu<sub>2</sub>Cl<sub>2</sub>O<sub>10</sub> (%): Cu, 16.63; F, 4.97. IR (KBr,  $\nu\text{ cm}^{-1}$ ): 1640 ( $\nu_{\text{C=N}}$ ), 1130, 1093 ( $\nu_{\text{ClO}_4}$ ), 626 ( $\delta_{\text{ClO}_4}$ ). The blue block crystals of [Cu<sub>2</sub>L](ClO<sub>4</sub>)<sub>2</sub> suitable for X-ray diffraction were obtained by slow diffusion of diethyl ether into the mother solution over one week.

**[Mn<sub>2</sub>L(H<sub>2</sub>O)<sub>2</sub>](ClO<sub>4</sub>)<sub>2</sub> (2).** 2 was prepared by a similar procedure as described above, except that the corresponding Mn(OAc)<sub>2</sub>·2H<sub>2</sub>O and Mn(ClO<sub>4</sub>)<sub>2</sub>·6H<sub>2</sub>O were used. Micro-crystals of [Mn<sub>2</sub>L(H<sub>2</sub>O)<sub>2</sub>](ClO<sub>4</sub>)<sub>2</sub> were obtained by slow diffusion of diethyl ether into the methanol solution of the crude product. Yield: 0.050 g, 46%. Anal.: found: Mn, 14.00; F, 4.89; Calcd for C<sub>24</sub>H<sub>28</sub>N<sub>4</sub>F<sub>2</sub>Mn<sub>2</sub>Cl<sub>2</sub>O<sub>12</sub> (%): Mn, 14.03; F, 4.85. IR (KBr,  $\nu\text{ cm}^{-1}$ ): 3400 ( $\nu_{\text{OH}}$ ), 1638 (C=N), 1131, 1090 ( $\nu_{\text{ClO}_4}$ ) and 619 ( $\delta_{\text{ClO}_4}$ ).

**[Ni<sub>2</sub>L(H<sub>2</sub>O)<sub>2</sub>](ClO<sub>4</sub>)<sub>2</sub> (3).** **3** was prepared by a similar procedure as described above, except that the corresponding Ni(OAc)<sub>2</sub>·2H<sub>2</sub>O and Ni(ClO<sub>4</sub>)<sub>2</sub>·6H<sub>2</sub>O were used. Yield: 0.069 g, 63%. Anal.: found: Ni, 14.80; F, 4.83; Calcd for C<sub>24</sub>H<sub>28</sub>N<sub>4</sub>F<sub>2</sub>Ni<sub>2</sub>Cl<sub>2</sub>O<sub>10</sub> (%): Ni, 14.84; F, 4.80; IR (KBr, ν cm<sup>-1</sup>): 3400 (ν<sub>OH</sub>), 1642 (C=N), 1131, 1092 (ν<sub>ClO<sub>4</sub></sub>) and 623 (δ<sub>ClO<sub>4</sub></sub>).

### 3. Results and discussion

#### 3.1. Synthesis and characterization

The presence of fluorine in the complexes presents the determination of C, H and N by elemental analyzer. The metals and fluorine contents were determined by general chemical methods. The acquired results agree with the compositions of the complexes.

In the infrared spectra of the complexes, the strong carboxyl absorption at 1694 cm<sup>-1</sup> in 2,6-diformylphenol disappeared, and sharp C=N stretching vibration bands corresponding to four imine groups of the macrocyclic framework are observed at 1641 cm<sup>-1</sup> for **1**, 1639 cm<sup>-1</sup> for **2** and 1636 cm<sup>-1</sup> for **3** [19]. The very strong bands centered at 1130, 1093 and 626 cm<sup>-1</sup>, 1131, 1090 and 619 cm<sup>-1</sup>, 1131, 1092 and 623 cm<sup>-1</sup> can be ascribed to ClO<sub>4</sub><sup>-</sup> vibration for **1**, **2** and **3**, respectively. The vibrations of ClO<sub>4</sub><sup>-</sup> in **1**, **2** and **3** exhibit well-defined split band centered at *ca* 1112 cm<sup>-1</sup>, implying that ClO<sub>4</sub><sup>-</sup> groups are coordinated to metal in the solid state [20].

The quality of the crystal of **2** and **3** are not good enough for structures by X-ray technique; the far-infrared spectra of **2** and **3** (figures 1 and 2) show characteristic bands for water in **2** at 570, 491 and 405 cm<sup>-1</sup>, ascribed to the two swaying vibrations of water and a stretch vibration of Mn–O (water), respectively. The bands at 466 and 299 cm<sup>-1</sup> correspond to stretch and deformational vibrations of Mn–O (phenoxide) in the macrocycle, and the similar vibration types of Mn–N are found at 392 and 228 cm<sup>-1</sup>. The band at 321 cm<sup>-1</sup> was designated as the Mn–O (perchlorate) stretch. In **3**, the swaying vibrations of water and stretch vibrations of Ni–O (water) appear at 566, 496 and 403 cm<sup>-1</sup> [21]. The bands found at 539, 351, 469, and 250 cm<sup>-1</sup> are ascribed to

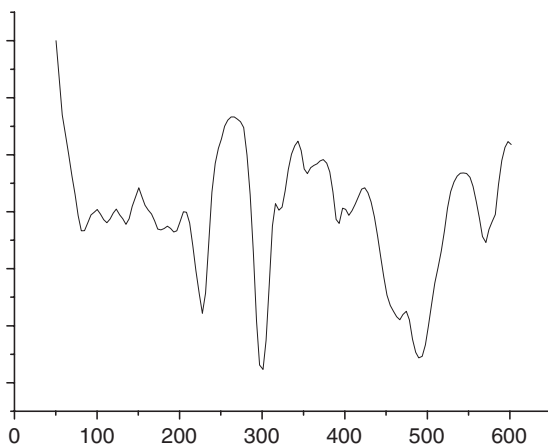


Figure 1. The far-infrared spectra of **2**.

the stretch and deformational vibrations of Ni–O (phenoxide) and Ni–N in the macrocycle [22], respectively. The results indicate that water and perchlorate were coordinated to the metal centers.

To prove water exists in **2** and **3**, thermogravimetric analyses of the complexes were done. In the thermogram of **1**, there is only one weight loss at about 260°C corresponding to decomposition of the complex with no weight loss from room temperature to 200°C, indicating no solvent water in **1**. Complexes **2** and **3** began to lose 4.61 and 4.70% of their weight at 105–115°C corresponding to the loss of two water molecules (Calcd, 4.60% for **2** and 4.55% for **3**), respectively. The results are consistent with IR spectra of the complexes. All complexes decomposed above 260°C.

### 3.2. Electrospray mass spectra

The ES-MS spectra of complexes **1**, **2** and **3** in MeOH solution are listed in table 1. For **1**, the ES-MS spectrum shows a peak corresponding to the macrocyclic coordinated ion  $[\text{Cu}_2\text{L}]^{2+}$  at  $m/z$  283.3 (100%), which confirms the formation of the complex, and another peak at  $m/z$  678.1 (60%) corresponding to  $[\text{Cu}_2\text{L}(\text{MeOH})_3(\text{OH})]^+$ . The results show that **1** is very stable in methanol solution. For **2**, the ES-MS spectrum gives a series of peaks at  $m/z$  631.1(100%), 613.3(95%), 634.1(48%) and 601.1(45%) corresponding to  $[\text{Mn}_2\text{L}(\text{MeOH})_{1.5}(\text{H}_2\text{O})(\text{OH})]^+$ ,  $[\text{Mn}_2\text{L}(\text{MeOH})_{1.5}(\text{OH})]^+$ ,  $[\text{Mn}_2\text{L}(\text{MeOH})(\text{H}_2\text{O})_2(\text{OH})]^+$  and  $[\text{Mn}_2\text{L}(\text{H}_2\text{O})_2(\text{OH})]^+$ , respectively. All species contain the dinuclear unit indicating that **2** is stable in methanol solution. Additionally, there are half solvent molecules in the series, demonstrating that some dimers exist in methanol solution with solvent molecules acting as  $\mu$ -bridges linking two macrocyclic complexes. The ES-MS spectrum of **3** shows peaks corresponding to the macrocyclic series  $[\text{Ni}_2\text{L}(\text{MeOH})_{1.5}(\text{H}_3\text{O})]^{3+}$ ,  $[\text{Ni}_2\text{L}(\text{ClO}_4)_{0.5}(\text{OH})_{0.5}]^+$ ,  $[\text{Ni}_2\text{H}_3\text{L}(\text{ClO}_4)_2]^{3+}$  and  $[\text{Ni}_2\text{H}_3\text{L}(\text{ClO}_4)_2(\text{MeOH})]^{3+}$  at  $m/z$  207.7(100%), 614.0(45%), 246.4(55%) and 263.7(35%), respectively. The behavior in the mass spectrum conditions is similar to that found for **2** with dimers of the macrocyclic complexes in solution.

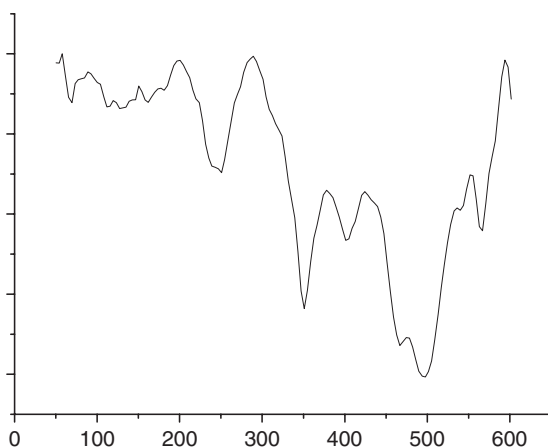


Figure 2. The far-infrared spectra of **3**.

### 3.3. Crystal structure of $[\text{Cu}_2\text{L}](\text{ClO}_4)_2$ (**1**)

The perspective view of  $[\text{Cu}_2\text{L}](\text{ClO}_4)_2$  (**1**) is given in figure 3, together with the atom numbering scheme. Crystallographic data and details about the data collection are presented in table 2. Selected bond lengths and angles for the copper(II) coordination are listed in table 3. The macrocyclic molecule has a symmetric center at the center of the Cu–Cu bond, and adopts a Z-shaped structure, similar to those reported by Thompson [23]. The planes of phenyls are parallel to each other with the parallel distance of 1.08 Å in the macrocycle. The angles between C=N and the phenyl connected with it are  $152^\circ$  and the same angles are found between the plane composed of  $\text{N}_4\text{O}_2$  and the phenyls in the complex. The coordination polyhedra of copper(II) ions are the same and could be described as a distorted octahedron with Jahn-Teller effects. Two oxygen atoms of each asymmetric bidentate perchlorate occupy the apical positions in a *trans*-arrangement with somewhat longer contacts 2.654 and 2.694 Å to copper(II), respectively, consistent with the infrared data, where three perchlorate vibrations are observed ( $1130, 1093, 626\text{ cm}^{-1}$ ), indicative of a low-symmetry

Table 1. The physical measurement of the complexes.

Complexes	Chemical analyses			ES-MS ( <i>m/z</i> , abundance)
	Metals	F		
<b>1</b>	Cu	16.58	5.01	283.3(100%), 678.1(60%)
<b>2</b>	Mn	14.00	4.89	631.1(100%), 613.3(95%), 634.1(48%), 601.1(45%)
<b>3</b>	Ni	14.80	4.83	207.7(100%), 614.0(45%), 246.4(55%), 263.7(35%)

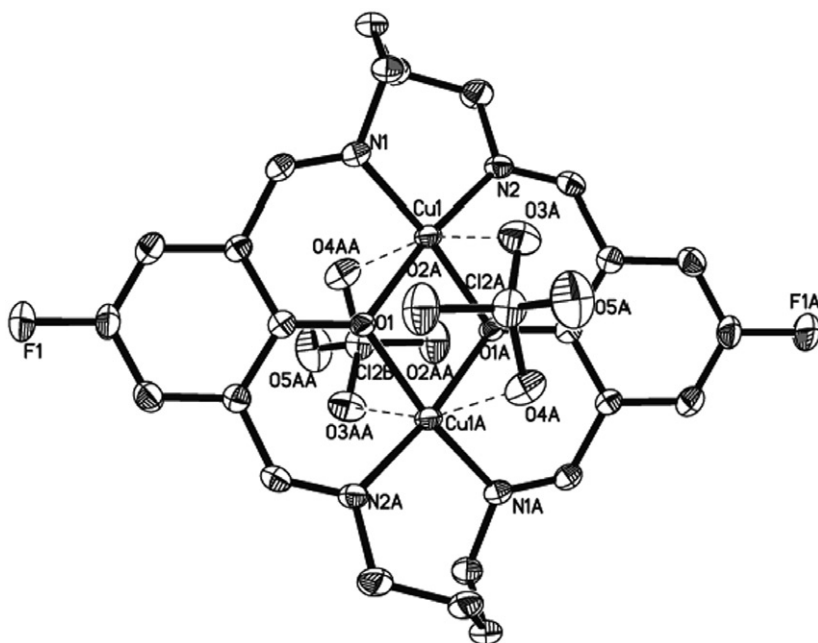


Figure 3. Perspective view of **1** with atom labels.

perchlorate. The copper–copper separation (3.042(3) Å) and phenoxide oxygen bridged angle (102.5(10)°) are comparable with those found in **1a** with a different substituent group (CH<sub>3</sub>) on the phenyl ring [23], the Cu–O (perchlorate) distances (2.654(3), 2.694(3) Å) are more similar and longer than those found in analogs [23]. The bidentate perchlorate coordination is similar to that found in **1a** and [Cu<sub>2</sub>(FPM)(ClO<sub>4</sub>)<sub>2</sub>] (FPM = **1a** with all azomethine nitrogens saturated) [23,24], except that the axial interactions are weaker and coordination of perchlorate is symmetric in [Cu<sub>2</sub>(FPM)(ClO<sub>4</sub>)<sub>2</sub>]. The distances between Cu(II) and coordinated atoms in the macrocycle fall in the range 1.935–1.960 Å. In-plane copper–oxygen distances (1.956(2) and 1.943(2) Å) are somewhat shorter than those in **1a** and copper–nitrogen distances (1.960(3) and 1.935(3) Å) are the same as those in **1a**, perhaps from the strong electron-withdrawing effect of the fluorine, increasing Cu → L. The copper departs by 0.0672 Å from the mean N<sub>2</sub>O<sub>2</sub> basal plane.

Table 2. Crystal data and details of the structure determination for complex **1**.

Empirical formula	C <sub>24</sub> H <sub>24</sub> Cl <sub>2</sub> N <sub>4</sub> Cu <sub>2</sub> O <sub>10</sub> F <sub>2</sub>
Formula weight	764.46
Crystal system	Orthorhombic
Space group	<i>Pbca</i>
<i>a</i> (Å)	15.4297(12)
<i>b</i> (Å)	10.1213(8)
<i>c</i> (Å)	17.6030(14)
$\alpha$ (°)	90
$\beta$ (°)	90
$\gamma$ (°)	90
Volume (Å <sup>3</sup> )	2749.0(4)
<i>Z</i>	8
<i>D</i> <sub>calcd</sub> (g cm <sup>-3</sup> )	1.814
$\mu$ (Moka) (nm)	1.638
<i>F</i> (000)	1536
Crystal size (mm <sup>3</sup> )	0.30 × 0.20 × 0.16
Temp. (K)	292 (2)
Mo–K $\alpha$ radiation (Å <sup>3</sup> )	0.71073
$\theta$ range (deg)	2.31–27.50
<i>N</i> <sub>ref</sub> , <i>N</i> <sub>par</sub>	3140, 199
Tot. uniq. data <i>R</i> (int)	17380, 3140, 0.0539
Observed data [ <i>I</i> > 2.0 $\sigma$ ( <i>I</i> )]	3140
<i>W</i> <sup>-1</sup>	1/[ <i>S</i> <sup>2</sup> ( <i>F</i> <sub>o</sub> <sup>2</sup> ) + (0.0403 <i>P</i> ) <sup>2</sup> + 1.7150 <i>P</i> ] <i>P</i> = ( <i>F</i> <sub>o</sub> <sup>2</sup> + 2 <i>F</i> <sub>c</sub> <sup>2</sup> )/3
<i>R</i> , <i>wR</i> <sub>2</sub> , <i>S</i>	0.0453, 0.1005, 1.050
Max. and Av. shift/error	0.001, 0.000
Min. and max. resd. dens. [e.Å <sup>-3</sup> ]	–0.472, 0.408

Table 3. Selected bond lengths (Å) and angles of complex **1**.

Bonds	Length (Å)	Bonds	Length (Å)
N1–Cu1	1.935(3)	Cu1A–O1	1.943(2)
Cu1–O1	1.956(2)	Cu1A–N2A	1.960(3)
Bond angles	Values (°)	Bond angles	Values (°)
N1A–Cu1A–O1	165.50(10)	N1A–Cu1A–O1A	90.52(10)
O1–Cu1A–O1A	77.46(10)	N1A–Cu1A–N2A	100.18(12)
O1–Cu1A–N2A	92.36(10)	Cu1–O1A–Cu1A	102.54(10)



### 3.4. Electrochemical properties of the complexes

The electrochemical properties of **1–3** have been studied by cyclic voltammetry in DMF containing 0.1 M tetra(*n*-butyl)ammonium perchlorate. A typical cyclic voltammogram of **1** in DMF is given in figure 4 and the numerical data of **1** and **3** summarized in table 4.

For **1**, when scanning from 0 to  $-1.2$  V, two cathodic peaks appeared at  $-0.492$  V and  $-0.168$  at scan rate  $0.02$  V s $^{-1}$ , corresponding to stepwise one-electron reductions of the binuclear copper(II) complex to a binuclear copper(I) species through a Cu(II)–Cu(I) intermediate. The reduction potentials are constant as the scan rate increases, revealing that the processes are controlled by the electrode reaction [25]. A comparison of the reduction potential (table 3) of the first one-electron-reduction steps for **1**, **1a** [23] and **1b** [26] (the derivative **1b** is *t*-butyl groups instead of fluorine in **1**) shows that the most thermodynamically favored process occurs for **1**, which not only has molecular flexibility associated with the butylene bridge similar to **1a**, but also a more positive copper(II) center associated with fluorine being the strong electron-drawing group, thus enhancing the stability of copper(I). The second one-electron-reduction step for this series also occurs at the most positive potential for **1**. These results indicate that the ring substituent electronic effects associated with fluoro (**1**), methyl (**1a**) and *t*-butyl (**1b**) groups influence the first and second one-electron reductions. The two waves for **1** were irreversible, poorly resolved anodic peaks, different from **1a** and **1b**. Thus, the strong electron withdrawing of fluorine increases absorption of the Cu(II)–Cu(I) and Cu(I)–Cu(I) species on the electrode. For **3**, when scanning from 0 to  $-1.5$  V, two pairs of anodic and cathodic peaks with the half-wave potentials ( $E_{1/2}$ )  $-1.142$  and  $-0.812$  V are observed. The cathodic and anodic peak currents that appeared at half-wave potentials ( $E_{1/2}$ )  $-0.812$  V are almost equal. The value of  $i_{pc}/\nu^{1/2}$  is constant as the scan rate varies between 50 and 150 mVs $^{-1}$ , indicating that the pseudo-reversible process with  $\Delta E = 103$  mV at  $\nu = 50$  mVs $^{-1}$  was controlled by diffusion. The second couple at  $-1.142$  V of the half-wave potential is also

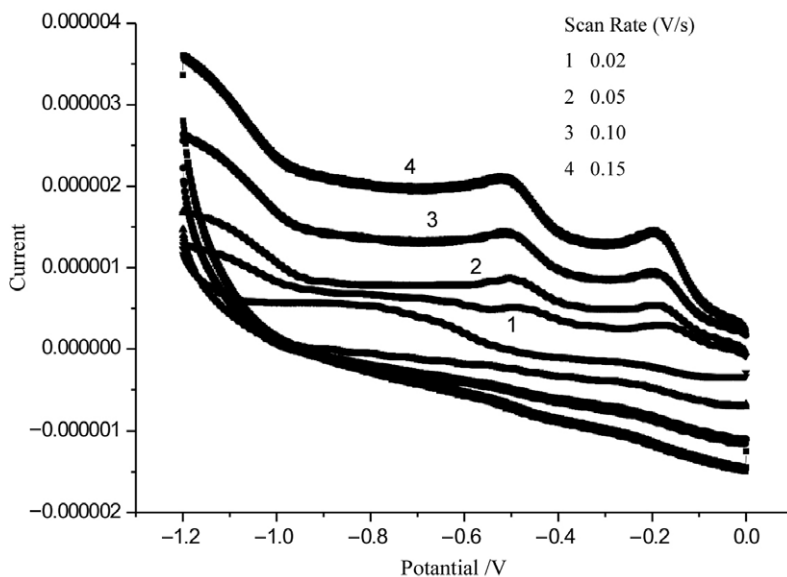


Figure 4. Cyclic voltammogram of **1** in DMF solution at different scan rates.

pseudo-reversible ( $\Delta E = 100$  mV). Compared with the analogs [27,28], the  $E_{1/2}$  for the first one-electron-reduction and the second-electron-reduction steps are all in the range  $-1.00 \sim 1.65$  V (first) and  $1.80 \sim 1.95$  V (second). The  $E_{1/2}$  value for the two steps in **3** is more positive than those of its analogs [27,28], similar to those found in the copper(II) complex described above. It can be concluded that metal centers are more positive when strong electron-withdrawing groups are attached to the ring of macrocyclic complexes and would be more easily reduced. There are no redox processes in the range  $0 \sim -1.5$  V for **2**.

### 3.5. Magnetic properties of (**1**)

The temperature dependence of magnetic susceptibility of **1** from 300 to 1.78 K is shown in figure 5 as  $\chi_M T$  versus  $T$  with nonlinear least-squares fitting of Bleaney–Bowers [29] equation (1) to the experimental data. The magnetic parameters of **1** can be estimated as  $g = 2.28$ ,  $-J = 542$  cm<sup>-1</sup>, and  $\rho = 0.00396$  with  $R = 1.008 \times 10^{-6}$  ( $R$  is an agreement factor defined as  $R = \sum [(\chi_M T)_{\text{Calcd}} - (\chi_M T)_{\text{obs}}]^2 / \sum (\chi_M T)_{\text{obs}}^2$ ), and so  $-2J = 1084$  cm<sup>-1</sup>, which indicates that relative strong antiferromagnetic coupling exists between the two copper(II) ions in **1**.

$$\chi = \frac{2Ng^2\beta^2}{kT} \times \frac{(1 - \rho)}{3 + \exp(-2J/kT)} + \frac{Ng^2\beta^2\rho}{kT} \quad (1)$$

In this expression,  $2J$  (in the spin Hamiltonian  $H = -2J\hat{s}_1\hat{s}_2$ ) is the singlet–triplet splitting or exchange integral,  $\chi$  and  $g$  have their usual meanings and  $\rho$  is the ratio of the paramagnetic impurity. According to the effective magnetism formula,  $\mu_{\text{eff}} = 2.828(\chi_M T)^{1/2}$ , the experimental effective magnetism quadrature equals  $0.42$  emu K mol<sup>-1</sup> at 290 K where  $\chi_M T = 0.0222$  emu K mol<sup>-1</sup>, which is much smaller than the theoretic value  $1.73$  emu K mol<sup>-1</sup> calculated from  $\mu_{\text{eff}} = g[S(S + 1)]^{1/2}$  (when  $g = 2.0$ ,  $S = 1/2$ ) based on the Cu(II) unit, indicating very strong interaction between two copper ions in the complex; similar magnetic behavior was observed for a structurally characterized analogous dicopper(II) complex [30,31]. The  $\chi_M T$  value rapidly decreases in the range 300–150 K, reaching a value  $1.008 \times 10^{-6}$  emu K mol<sup>-1</sup>, and is then constant in the range 150–10 K. The result agrees well with the crystal structure of **1**, in which the distance (3.042 Å) of two copper(II) is much shorter than its analogues.

Comparing coordination structures of **1** with that of **1a**, the average phenoxide-bridged angle and the average Cu–O (bridge) distance in **1** are slightly smaller than those in **1a**, and the solid angle at the phenoxide bridge in **1** ( $355.94^\circ$ ) is slightly larger than that

Table 4. Cyclic voltammogram data for the complex **1**, **2**, **1a**, **1b** and **2** (scan rate 100 mV s<sup>-1</sup>).

Complex	Redox potential (V)			
	$E_{\text{pc}} (E_{\text{pa}})$	$E_{1/2}$	$E_{\text{pc}} (E_{\text{pa}})$	$E_{1/2}$
<b>1</b>	-0.492		-0.168	
<b>1a</b>	-0.810 <sup>a</sup>		-0.350 <sup>a</sup>	
<b>1b</b>	-0.922 <sup>b</sup>		-0.530 <sup>b</sup>	
<b>2</b>	-1.192(-1.092)	-1.142	-0.864(0.761)	-0.812

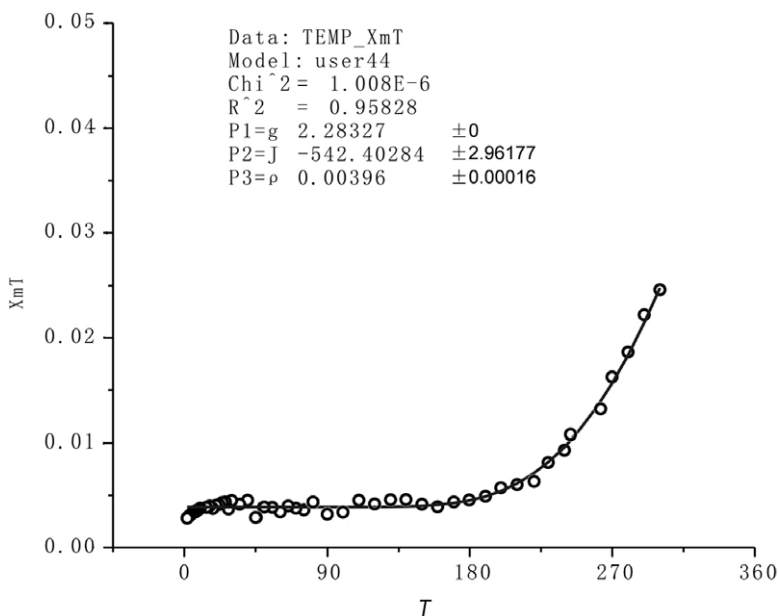


Figure 5. Experimental and calculated plots of  $\chi_M T$  (emu K mol<sup>-1</sup>) vs.  $T$  (K). The solid line shows the fit with the equation (1).

in **1a** (353.17°); pyramidal distortion is almost the same. The coordination polyhedra of **1** and **1a** are much the same. Spin exchange between copper(II) centers bridged by oxygen donors are dependent upon the degree of pyramidal distortion at the oxygen bridge [23,31]. However, the  $2J$  for **1** (1084 cm<sup>-1</sup>) is much greater than that for **1a** (850 cm<sup>-1</sup>) despite the fact that there are similar coordination structures in the Cu<sub>2</sub>O<sub>2</sub>N<sub>2</sub> centers. So the difference of the exchanges ( $2J$ ) between **1** and **1a** can be attributed to the electronic effects of substituents in the macrocyclic ring. Because of the increased charge on copper(II) caused by the strong electron-withdrawing fluorine, the antiferromagnetic exchange is enhanced in **1**, in agreement with the electrochemical data.

#### 4. Conclusion

Three macrocyclic complexes ([M<sub>2</sub>L(H<sub>2</sub>O)<sub>*n*</sub>](ClO<sub>4</sub>)<sub>2</sub>, M = Cu, Mn, Ni;  $n = 0, 2$ ) have been obtained by (2 + 2) cyclocondensation between 2,6-diformyl-4-fluorophenol and 1,4-diaminobutane in the presence of M<sup>2+</sup> ions. The crystal structure shows that **1** adopts a Z-shaped structure with Cu–Cu separation 3.042 Å bridged by phenoxo groups. The coordination polyhedra of the two copper(II) are distorted octahedra. The ES-MS, thermogravimetric analyses and far-infrared spectra confirm that **1** does not contain coordinated waters, while **2** and **3** contain two coordination waters. The results of cycle voltammograms show that **1** has only two reduction processes, while **3** has two couples of redox processes. Variable-temperature magnetic susceptibility data for **1** reveal strong antiferromagnetic interactions with the magnetic parameters  $g = 2.28$ ,  $J = -542.4$  cm<sup>-1</sup>, and  $\rho = 0.00396$ . The strong electron-withdrawing fluorine

in the phenyl ring enhances the antiferromagnetic exchange of the complex and makes it more easily reduced than its analogs.

## Acknowledgement

The project was supported by the National Nature Science Foundation of China [20271039].

## References

- [1] P.A. Vigato, S. Tamburini. *Coord. Chem. Rev.*, **248**, 1717 (2004).
- [2] H. Ōkawa, H. Furutachi, D.E. Fenton. *Coord. Chem. Rev.*, **174**, 51 (1998).
- [3] B. Ramachandran, K. Ravi, V. Narayanan, M. Kandaswamy, S. Subramanian. *Clin. Chim. Acta*, **345**, 141 (2004).
- [4] S. Koner, S. Saha, K.I. Okamoto, J.P. Tuchagues. *Inorg. Chem.*, **42**, 4668 (2003).
- [5] N. Sabbatini, M. Guardingli, J.M. Lehn. *Coord. Chem. Rev.*, **123**, 201 (1993).
- [6] J. Nishio, H. Ōkawa, S.I. Ohtsuka, M. Tomono. *Inorg. Chim. Acta*, **218**, 27 (1994).
- [7] H. Ōkawa, J. Nishio, M. Ohba, M. Tadokoro, N. Matsumoto, M. Koikawa, S. Kida, D.E. Fenton. *Inorg. Chem.*, **32**, 2949 (1993).
- [8] M. Tadokoro, H. Ōkawa, N. Matsumoto, M. Koikawa, S. Kida. *J. Chem. Soc., Dalton Trans.*, 1657 (1991).
- [9] H. Ōkawa, H. Furutachi, D.E. Fenton. *Coord. Chem. Rev.*, **174**, 51 (1998).
- [10] J. Wang, X.Y. Xu, J.L. Chen, Q.H. Luo, M.C. Shen, X.Y. Huang, Q.J. Wu. *Inorg. Chim. Acta*, **256**, 121 (1997).
- [11] B.K. Wagon, S.C. Jackels. *Inorg. Chem.*, **28**, 1923 (1989).
- [12] L. Sabatini, L. Fabbrizzi. *Inorg. Chem.*, **18**, 438 (1979).
- [13] C.R.K. Rao, P.S. Zacharias. *Polyhedron*, **16**, 1201 (1997).
- [14] H. Zhou, Z.H. Peng, Z.Q. Pan, D.C. Li, B. Liu, Z. Zhang, R.A. Chi. *J. Mol. Struct.*, **743**, 59 (2005).
- [15] B. Liu, H. Zhou, Z.Q. Pan, H.P. Zhang, J.D. Hu, X.L. Hu. *Trans. Met. Chem.*, **30**, 1020 (2005).
- [16] H. Zhou, Z.H. Peng, Z.Q. Pan, B. Liu, X.L. Hu, Y.Q. Liu. *J. Coord. Chem.*, **58**, 443 (2005).
- [17] Smart and Saint. Area Detector Control and Integration Software, Siemens Analytical X-Ray Systems, Inc., Madison, Wisconsin, USA (1996).
- [18] G.M. Sheldrick. *SHELXTL V5.1 Software Reference Manual*, Bruker AXS, Inc., Madison, Wisconsin (1997).
- [19] H. Okawa, S. Kida. *Bull. Chem. Soc. Jpn*, **45**, 1759 (1972).
- [20] K. Nakamoto. *Infrared and Raman Spectra of Inorganic and Coordination Compounds*, 3rd Edn, Wiley-Interscience, New York (1977).
- [21] G. Blyhoder, N. Ford. *J. Phys. Chem.*, **68**, 1496 (1964).
- [22] D.M. Adam, D.C. Stevens. *Inorg. Chem.*, **20**, 525 (1981).
- [23] S.K. Mandal, L.K. Thompson, M.J. Newlands, E.J. Gabe. *Inorg. Chem.*, **28**, 3707 (1989).
- [24] S.K. Mandal, L.K. Thompson, K. Nag, J.P. Charland, E.J. Gabe. *Inorg. Chem.*, **26**, 1391 (1989).
- [25] S. Mohanta, S. Baitalik, S.K. Dutta, B. Adhikary. *Polyhedron*, **17**, 2669 (1998).
- [26] R.C. Long, D.N. Hendrickson. *J. Am. Chem. Soc.*, **105**, 1513 (1983).
- [27] Y. Aratake, M. Ohba, H. Sakiyama, M. Tadokoro, N. Matsumoto, H. Ōkawa. *Inorg. Chim. Acta*, **212**, 183 (1993).
- [28] J. Niahio, H. Ōkawa, S.I. Ohtsuka, M. Tomono. *Inorg. Chim. Acta*, **218**, 27 (1994).
- [29] B. Bleaney, K.D. Browsers. *Prog. R. Soc. London, Ser. A*, **214**, 415 (1952).
- [30] I.K. Thompson, S.S. Mandal. *Inorg. Chem.*, **35**, 3117 (1996).
- [31] S. Mohanta, S. Baitalik, S.K. Dutta. *Polyhedron*, **17**, 2669 (1998).